ELSEVIER

Polymer 42 (2001) 6119–6127

polymer

www.elsevier.nl/locate/polymer

Precipitation of Nylon 6 membranes using compressed carbon dioxide

Yeh Wei Kho[a], Douglass S. Kalika[a,b], Barbara L. Knutson[a,*]

[a]*Department of Chemical and Materials Engineering, University of Kentucky, 177 Anderson Hall, Lexington, KY 40506-0046, USA*
[b]*Center for Robotics and Manufacturing Systems, University of Kentucky, Lexington, KY 40506-0108, USA*

Received 5 September 2000; received in revised form 8 January 2001; accepted 8 January 2001

Abstract

Membrane formation using a compressed antisolvent is analogous to conventional immersion precipitation using liquid nonsolvents and introduces pressure as an additional variable for tailoring the membrane microstructure. Thin films of a semicrystalline polyamide, Nylon 6, were precipitated from 2,2,2-trifluoroethanol by exposing the incipient membrane to compressed CO_2 antisolvent at 35°C and variable pressures up to 173.4 bar. Membrane structures dominated by liquid–liquid (L–L) and solid–liquid (S–L) demixing processes were observed as a function of precipitation conditions. Interpretation of the resulting membrane morphologies was based on structural features observed for traditional phase inversion processes and reflected the relative rates of L–L and S–L demixing as a function of the pressure-dependent strengths of the solvent and antisolvent. The ability to tailor the morphology of a semicrystalline membrane using compressed antisolvent suggests an alternative to current CO_2-based polymer impregnation techniques, which require solute solubility in CO_2, for the generation of composite thin films and membranes.

Keywords: Nylon 6; Compressed CO_2; Membrane formation

1. Introduction

Compressed or supercritical fluids are finding increasing application as solvents for polymer processing based on their ability to achieve desirable morphologies while eliminating or reducing the use of traditional organic solvents. Precipitation from droplets using a compressed antisolvent (PCA), for example, has been used to generate monodisperse, sub-micron microspheres of biodegradable polymers with potential application to controlled drug release [1–3]. Additional structures such as porous fibers and microfibers have been obtained by altering the conditions at which the dissolved polymer is contacted with the compressed antisolvent [4–6]. Compressed antisolvent processes, which commonly employ CO_2, make use of the low solubility of most high molecular weight molecules in compressed or supercritical CO_2 and the high mutual affinity of CO_2 for a range of organic solvents. General advantages of PCA include the ability to tune the antisolvent strength with temperature and pressure, the recovery of a dry polymeric product following depressurization, and the ease of organic solvent recovery relative to traditional liquid–liquid nonsolvent processes. Compressed or supercritical CO_2 ($T_c = 31.1$°C, $P_c = 73.8$ bar) offers the additional benefits of being nonflammable, nontoxic, environmentally acceptable, inexpensive and having a mild critical temperature for the processing of thermally-labile compounds.

PCA is characteristically a rapid precipitation process resulting in high product yield. The simultaneous diffusion of the antisolvent into the organic phase and the evaporation of the organic solvent into the bulk antisolvent are enhanced by the gas-like diffusivities of the near-critical fluid and the density reduction of the expanded organic phase [5]. This rapid precipitation process has been used to obtain novel bulk morphologies (such as monodisperse sub-micron particles) as well as nonequilibrium molecular-level morphologies (e.g. in immiscible polymer blends [7]).

Although PCA is typically conducted by spray contacting the dissolved solute and the compressed antisolvent, the potential to obtain unique thin film and membrane morphologies suggests the utility of *casting* dissolved polymeric solutions in the presence of a compressed antisolvent. Several aspects of this process to the potential variation of morphology: the rapidity of the precipitation process, the tendency of compressed CO_2 to swell and plasticize polymers, and the ability to quickly depressurize the system to lock in a structure. The latter two phenomena have been employed to foam polymers [8], blend polymers [9], and impregnate solutes in polymeric films [10,11] in the presence of compressed CO_2. Thus compressed CO_2 may

* Corresponding author. Tel.: +1-859-257-5715/8028; fax: +1-859-323-1929.
E-mail address: bknutson@engr.uky.edu (B.L. Knutson).

0032-3861/01/$ - see front matter
PII: S0032-3861(01)00067-2

provide a flexible and benign environment for membrane formation and the subsequent modification of the film.

Membrane formation using a compressed antisolvent is analogous to traditional phase inversion membrane formation by immersion precipitation. Immersion precipitation consists of casting a thin film of the dissolved polymer on an inert substrate and immersing this substrate in a bath containing a nonsolvent with respect to the polymer. Rapid exchange of the solvent and nonsolvent results in diffusion-induced phase separation, and ultimately membrane formation. The time scale of this two-way mass transfer dictates the demixing mechanisms that are accessible to the polymer/solvent/nonsolvent system. The resulting morphology is largely determined by the dominant demixing process at the onset of membrane formation [12]. Polymer/solvent/nonsolvent phase diagrams have been used to interpret membrane morphology as a function of precipitation conditions in traditional liquid immersion precipitation processes, with appropriate consideration of kinetic factors as well [13]. The presence of structural gradient features, such as a dense nonporous top layer, is often strongly indicative of the time scale of demixing (i.e. delayed versus instantaneous demixing) [14].

The ability to vary membrane pore size, pore structure, crystallinity, and gradient features is crucial for the tailoring of selectivity and permeability to specific applications. In immersion precipitation, variables traditionally used to control membrane morphology include the composition of the casting solution, the strength of the nonsolvent bath, and the precipitation temperature. The substitution of compressed or supercritical fluid for the traditional liquid nonsolvent phase allows for the tuning of antisolvent strength (density) by means of pressure. Thus, the use of a compressed or supercritical fluid antisolvent introduces the pressure of the antisolvent phase as an additional variable by which to influence the demixing process and control the membrane morphology.

This paper examines our ability to vary morphology in flat-sheet membranes as a function of processing conditions using compressed CO_2 as an antisolvent. The polymer chosen for this study, Nylon 6, is a rapidly crystallizing aliphatic polyamide. The solvent and antisolvent used were 2,2,2-trifluoroethanol and compressed carbon dioxide (CO_2), respectively. Phase equilibria of this ternary system have been shown to exhibit both liquid–liquid (L–L) and solid–liquid (S–L) demixing [15]; in addition, CO_2 is completely miscible in TFE at temperatures between 298 and 373 K and pressures ranging from 1 to 400 bar [15]. The solubility of Nylon 6 in CO_2 at the same conditions is negligible, making CO_2 an appropriate antisolvent for Nylon 6/TFE solution. The polymer/solvent/antisolvent system was chosen so as to maximize the potential for producing membranes with both L–L and S–L demixing characteristics, and to investigate the feasibility of altering the dominant demixing mechanism with variations in pressure and pressure profile (see Section 2.2). The morphology of these membranes is interpreted using descriptions that parallel the analysis of morphological features observed for traditional phase inversion membranes.

2. Materials and methods

2.1. Materials

Nylon 6 was obtained from Aldrich Chemical in pellet form. Nylon 4,6 was obtained through the courtesy of DSM Engineering Plastics, also in pellet form. The solvent, 2,2,2-trifluoroethanol, (99.5 + %, NMR Grade; density 1.373 g/ml) was purchased from Aldrich Chemical. High purity carbon dioxide (99.99%) was obtained from AGA Specialty Gas. Ultra high purity grade nitrogen was purchased from Scott-Gross Co. Inc.. All reagents were used without any further purification.

2.2. Experimental procedures

Nylon 6 and Nylon 4,6 pellets were dried in vacuo at approximately 80°C and placed in a desiccator prior to use. A 15 wt% Nylon 6 polymer solution was prepared by dissolving an appropriate amount of Nylon 6 pellets in 2,2,2-trifluoroethanol. The mixture was capped and stirred with a magnetic stir bar overnight to ensure dissolution. A thin film was cast onto a glass microscope slide using a Doctor's blade at conditions that resulted in a final membrane thickness ranging from 150 to 250 μm. The casting process was performed in a self-constructed glove box purged with nitrogen gas to avoid contact of the polymer with ambient humidity. After the film was cast, the glass slide was immediately transferred to a pressure vessel (Fig. 1; 100 ml Parr® Series 4590 Micro Reactor) and assembled in a glove box. After the pressure vessel was sealed under nitrogen environment, CO_2 was introduced into the reactor

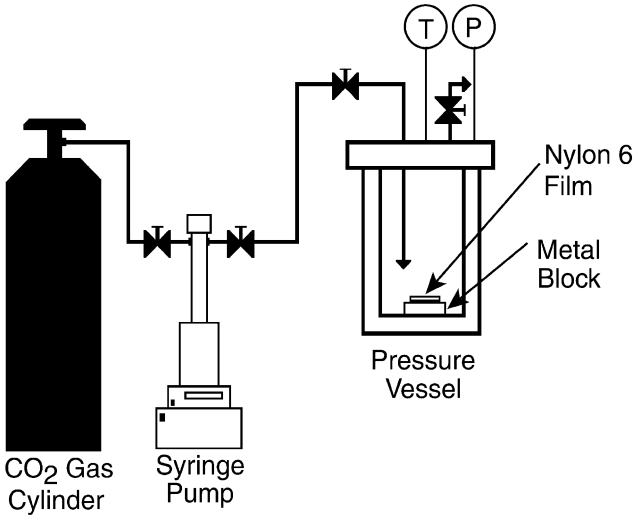

Fig. 1. Schematic view of the experimental set-up used for the formation of nylon membranes in the presence of compressed CO_2.

at 6.9 bar/min using a syringe pump (ISCO® Model 500D). The temperature of the pressure vessel was controlled by a Parr® Model 4842 PID controller and held at approximately 35°C throughout all of the experiments in this study. After the desired pressure was reached, it was held for 30 min. At the end of the experiment, the vessel was depressurized at a rate of approximately 6.9 bar/min. As soon as the depressurization process was completed, the resulting white, opaque membrane was collected from the pressure vessel.

Two distinct variations of this technique were as follows: (i) preconditioning of the cast solution in the presence of compressed CO_2 at reduced pressure and (ii) casting and precipitation of the membrane in the presence of liquid TFE in the pressure vessel. The first variation, preconditioning with CO_2, involved ramping the CO_2 pressure at a constant rate to a level below that required for membrane formation (28.6 bar or 56.2 bar), holding at this conditioning pressure for 30 min, and then increasing the system pressure to the final desired value. The second variation, casting in the presence of liquid TFE, required the introduction of approximately 1 ml TFE into the bottom of the vessel prior to closure and pressurization. A standard pressure cycle was then used to form the membrane, as described above.

The membranes were prepared for SEM analysis by first fracturing them in liquid nitrogen. The fractured membrane samples were then mounted vertically on aluminum stubs using double adhesive carbon conductive tabs (Ted Pella) and coated with Ni in an Emscope SC400 sputter-coater under an Ar atmosphere. A Hitachi S-3200N scanning electron microscope (SEM) at an accelerating voltage of 10 kV was used to obtain digital images of the samples. Care was taken in membrane handling and mounting in order to clearly distinguish between the top surface of the membrane (surface in contact with the antisolvent phase) and the bottom surface of the membrane (surface in contact with the glass substrate). The SEM micrographs presented below depict representative samples from duplicate runs for each experimental condition.

3. Results and discussion

The morphology of phase inversion membranes is governed by the simultaneous thermodynamic and kinetic events that lead to precipitation. These events can be represented by mass transfer pathways overlaid on a ternary phase diagram (see Fig. 2) [14,16–17]; this approach and its underlying assumptions have been reviewed extensively by van de Witte and coworkers [17]. Assuming an infinite film thickness, the mass transfer pathways reflect both the composition of a specific element in the cast solution as a function of time as well as the range of compositions across the cast solution (i.e. from the film-nonsolvent interface to the support) [17]. As shown in Fig. 2, the representative mass transfer pathways can provide a qualitative description

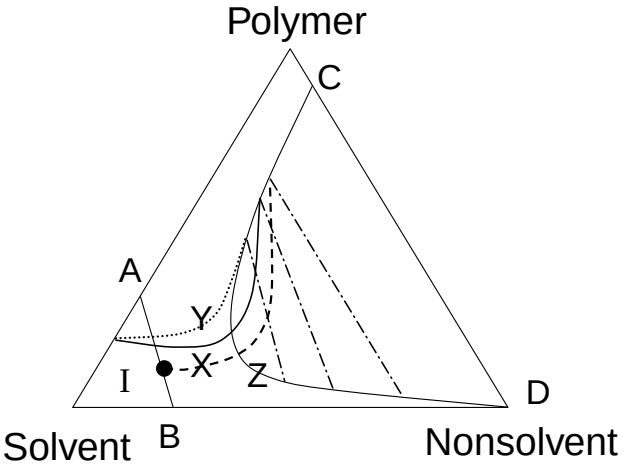

Fig. 2. Schematic representation of possible demixing mechanisms during membrane formation. Region I: Homogeneous solution. Line AB: S–L demixing boundary. Line CD: Binodal envelope. Tie line (— – —). Path X (——): Composition path showing the composition of the nascent membrane crossing the binodal envelope under strong nonsolvent conditions, inducing instantaneous demixing; Path Y (·····): Composition path suggesting a formation mechanism dominated by crystallization (S–L demixing), typically occurring in 'soft' baths that favor delayed demixing; Path Z (- - - - -): Composition path for a metastable casting dope, as indicated by the composition of the solution near the support (●) (adapted from [17]).

of the effect of initial polymer casting concentration and solvent and nonsolvent strength on the precipitation events and resulting membrane morphology [17].

The morphological features observed in semicrystalline polymeric membranes formed by phase inversion techniques often reflect competition between L–L demixing, leading to smooth, cellular pores; and S–L demixing, leading to jagged or spiny structures that are more interconnected in nature. The dominant precipitation mechanism is not necessarily the one that is thermodynamically favored [13], and this highlights the interplay between the kinetic and thermodynamic processes operative during membrane formation. For example, precipitation may result from L–L demixing even though crystallization is more thermodynamically favored [18], as represented by composition pathway X in Fig. 2. Although some portion of the incipient membrane is metastable with respect to crystallization, compositions in the L–L two-phase region are reached via rapid mass transfer before the polymer chains are able to crystallize. In general, the resulting morphologies can be the product of simultaneous L–L and S–L demixing, or a variety of crystalline-shaped substructures captured at different stages of morphological development [19–21].

The demixing processes described above result in the porosity associated with membrane structures. In addition, uniform dense films of the polymer can be formed by evaporation of the solvent directly into the external phase. From initial experiments, it was observed that a porous membrane could not be formed below a CO_2 pressure of 56.2 bar. Instead, a dense film was formed, consistent with

the evaporation of the solvent (TFE) into the compressed CO_2 vapor phase. The pressurization, venting, and depressurization procedures for these experiments were identical to those used in subsequent higher pressure studies, and it is unclear which step of the cycle was responsible for the solvent evaporation. However, this result indicates that the compressed CO_2 lacked the strength to be an effective antisolvent at pressures below ~56.2 bar. As such, it can be concluded that the features obtained by exposure to higher CO_2 pressures were due primarily to the phase inversion that occurred at these elevated pressures, and were not formed during the subcritical ramping step.

The potential exists for additional processes that might alter membrane structure after initial formation e.g. CO_2-induced crystallization of the polymer, or CO_2-assisted-foaming during depressurization. CO_2-induced crystallization has been reported for polymers such as polycarbonate, polystyrene, poly(aryl ether ether ketone) and poly(ethylene terephthalate) [22–25], and the properties of CO_2 as a foaming agent have been exploited to produce microcellular polymeric foams, primarily of amorphous polymers [8]. Several experiments were performed to ensure that such post-formation processes did not significantly influence the membrane structures observed in our studies. The possible occurrence of additional, CO_2-induced crystallization after membrane formation was investigated by varying the sample hold time at elevated pressure. No evidence of additional or altered crystalline microstructure was observed in these experiments. The ability of CO_2 to foam films of semicrystalline Nylon 6 was examined by forming dense films of the polymer by evaporation, exposing these films to high pressure CO_2 (104.4 bar) for either 30 min or 15 h, and then rapidly depressurizing over 10 min. Neither sample exhibited any evidence of foaming as a result of the CO_2 exposure and rapid depressurization.

The membrane pore structure, gradient features, and surface characteristics were interpreted as a function of the rate and extent of CO_2 pressurization for each membrane formed. The properties of a Nylon 6 membrane precipitated from a 15 wt% casting solution at a pressurization rate of 6.9 bar/min (final pressure = 104.4 bar) served as a reference for comparison of membrane features as a function of precipitation conditions. System temperature was nominally 35°C, although the temperature was not well-controlled during the pressurization and depressurization processes, and ranged between 28 and 40°C. The various experimental conditions and corresponding membrane micrographs are outlined in Table 1.

The cross section of a membrane formed at the reference conditions (constant pressurization rate to a final pressure of 104.4 bar) displays a uniform structure comprised of cellular pores with a diameter of approximately 0.4 microns (Fig. 3a and b). This structure indicates L–L demixing as the dominant mechanism of membrane formation. The fine spiny structures at the periphery of the pores suggest that crystallization rapidly followed the L–L demixing, locking in the cellular structure (Fig. 3b). Similar observations of initial L–L nucleation and growth, followed by crystallization have been reported for immersion precipitation membranes prepared form rapidly crystallizing polylactides [26]. The membrane top surface displays an even distribution of (0.4 μm) pores (Fig. 3c), again consistent with L–L demixing as the dominant mechanism of membrane formation.

The absence of gradients over the cross section of the membranes provides insight as to the relative rates of mass transfer during membrane formation. The membranes cast in the presence of compressed CO_2 lacks a dense skin layer at the top surface. This is consistent with a delayed demixing process at the film-antisolvent interface [14], as opposed to instantaneous demixing as is typically encountered in the presence of a strong antisolvent phase. Membranes formed by instantaneous demixing are characterized by markedly asymmetric cross sections, and may display nodular toplayers [27–28], as well as large macrovoids in the membrane substructure. None of these features associated with rapid demixing were observed for the membrane formation conditions studied here.

The lack of structural gradients in the membranes formed with compressed CO_2 suggests rapid diffusion of the antisolvent into the solvent–polymer cast, with the formation of a uniform metastable liquid film prior to the onset of demixing. This may be influenced to some degree by the pressurization process itself, which is not instantaneous and which is limited by the experimental apparatus. The membrane precipitation time scale in the metastable film is sufficiently rapid to favor L–L demixing, and the emergence of a cellular morphology prior to the onset of crystallization.

The membrane produced by increasing the final system pressure to 173.4 bar (Fig. 4) is similar to the membrane generated at 104.4 bar (Fig. 3). Although the pore sizes are comparable, the cellular character of the membrane produced at higher pressure is somewhat more pronounced. Previous investigators have observed that strong antisolvent conditions favor L–L demixing in rapidly crystallizing polymer systems [19]. The observed increase in L–L demixing characteristics for membranes generated at higher pressures is consistent with the increased antisolvent strength of CO_2 at these pressures.

The failure to observe more significant changes in membrane structure with final pressure may be a reflection of two factors. First, Nylon 6 is a rapidly crystallizing polymer, and the potential variation in crystallization time scale with nonsolvent strength may be too small to affect an observable change in membrane structure. Second, pressurization is limited to ~7 bar/min, due to the constraints of the experimental apparatus. Therefore, the membranes were, in fact, subjected to a gradual change in the antisolvent strength as the final pressures were approached, and the full impact of that change on the demixing mechanism may be reduced as compared to an instantaneous pressurization.

Table 1
Experimental conditions and resulting membrane morphologies as observed by scanning electron microscopy

Fig. no.	Final hold pressure (bar)	Preconditioning pressure (bar)	Excess TFE	Membrane morphology (SEM)	Dominant demixing mechanism
3	104.4	–	No	Cellular pores	L–L
4	173.4	–	No	Cellular pores	L–L
5	104.4	28.6	No	Tighter pores; decreased pore interconnectivity	L–L
6	104.4	56.2	No	Pores with increased interconnectivity	L–L
7	104.4	28.6	Yes	Large crystallites	S–L
8[a]	104.4	–	No	Small, cellular pores	L–L

[a] Membrane formed from 9 wt% Nylon 4,6 solution in TFE; precipitated in an antisolvent environment of 104.4 bar.

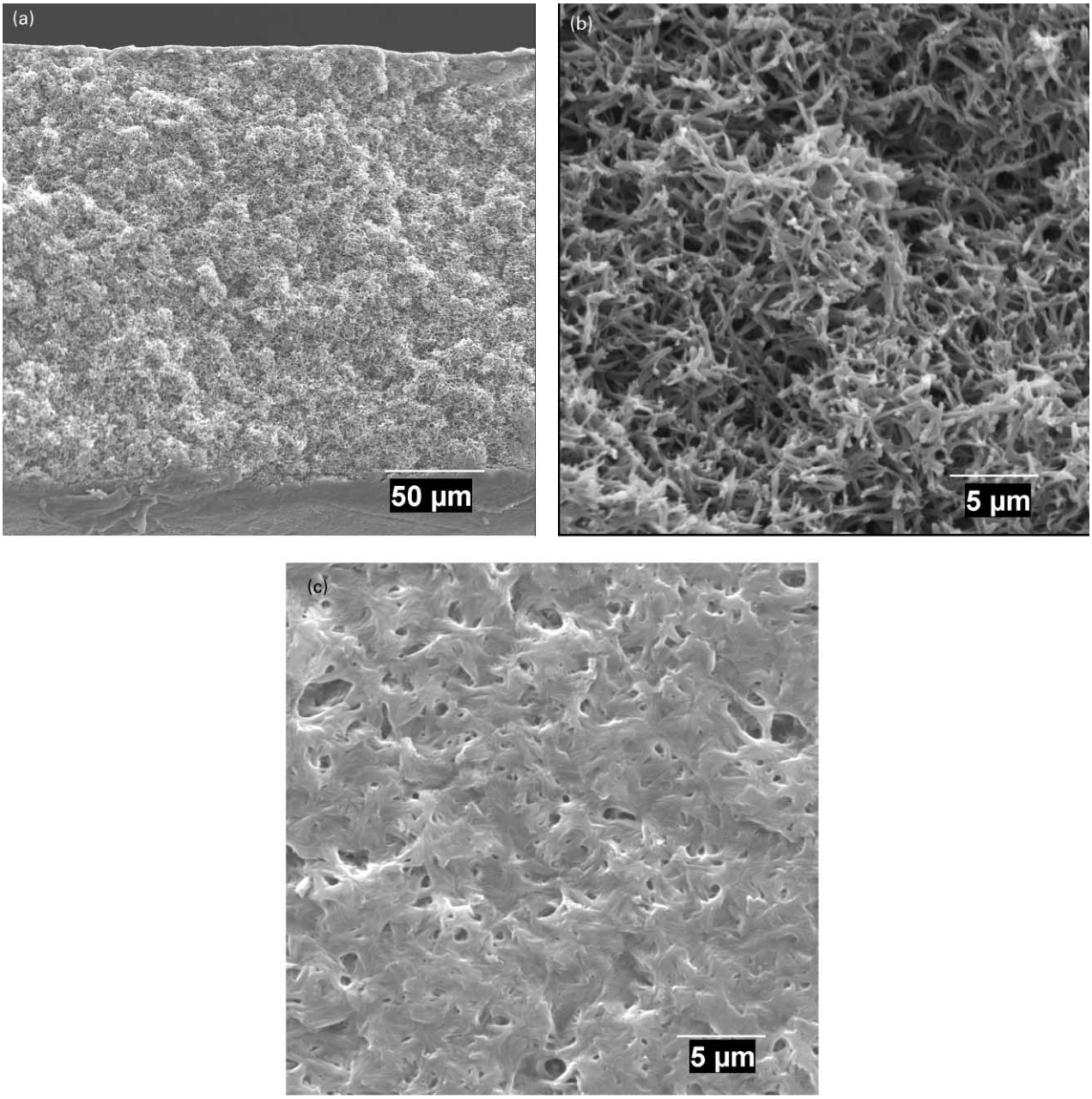

Fig. 3. SEM micrographs of a semicrystalline membrane formed from 15 wt% Nylon 6 solution in 2,2,2-trifluoroethanol (TFE); precipitated in an antisolvent environment of 104.4 bar CO_2. (a) cross section, 450×. (b) cross section, 4000×. (c) top surface, 4000×.

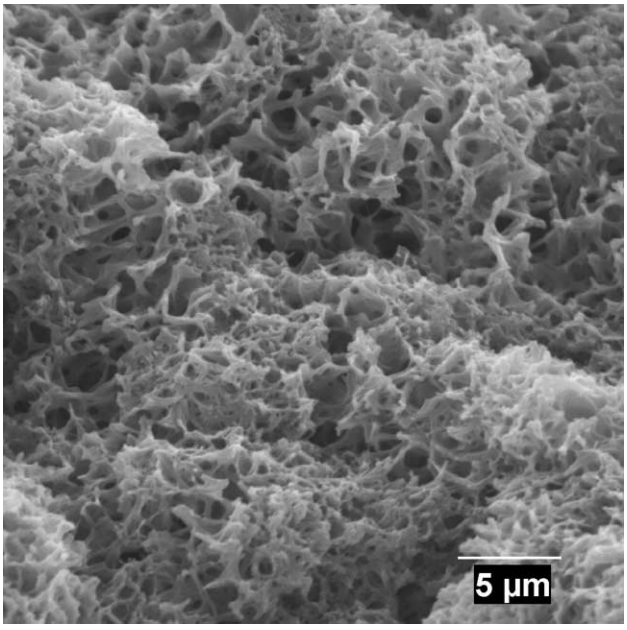

Fig. 4. SEM micrograph of Nylon 6 membrane precipitate in an antisolvent environment of 173.4 bar CO_2 (cross section, 4000×).

Changing the solvent strength of the casting solution through the addition of a small amount of nonsolvent is a technique used to manipulate the microstructure of membranes formed by phase inversion. Preconditioning cast films at a CO_2 pressure below the precipitation pressure represents the equivalent modification of solvent strength for CO_2-induced membrane formation. The effect of preconditioning on membrane formation was investigated by exposing cast films to pressurized CO_2 at 28.6 or 56.2 bar for 30 min prior to pressurization to the final conditions. The pressure profile for these preconditioned membranes consisted of (a) increasing the CO_2 pressure to 28.6 or 56.2 bar at a constant rate of 6.9 bar/min, (b) maintaining this intermediate pressure for 30 min, and (c) ramping to the final pressure of 104.4 bar and holding for 30 min before depressurization and recovery of the membrane.

The effect of preconditioning at 28.6 bar prior to final pressurization to 104.4 bar is shown in Fig. 5a. The preconditioned membrane has a tighter pore structure than the corresponding film formed by direct pressurization (refer to Fig. 3b); the preconditioned membrane is characterized by decreased pore interconnectivity and a less cellular structure. The top surface of the preconditioned membrane (Fig. 5b) has tighter pores and a higher pore density relative to the membrane formed by direct pressure ramping (Fig. 3c). In contrast, a preconditioning pressure of 56.2 bar (Fig. 6a and b) results in a pore structure similar to that obtained by direct pressurization, with greater cellular character and pore interconnectivity. Increasing the final system pressure to 173.4 bar in conjunction with the respective preconditioning pressures had no apparent effect on the membrane structure (SEM micrographs not shown).

Membrane formation following conditioning with low

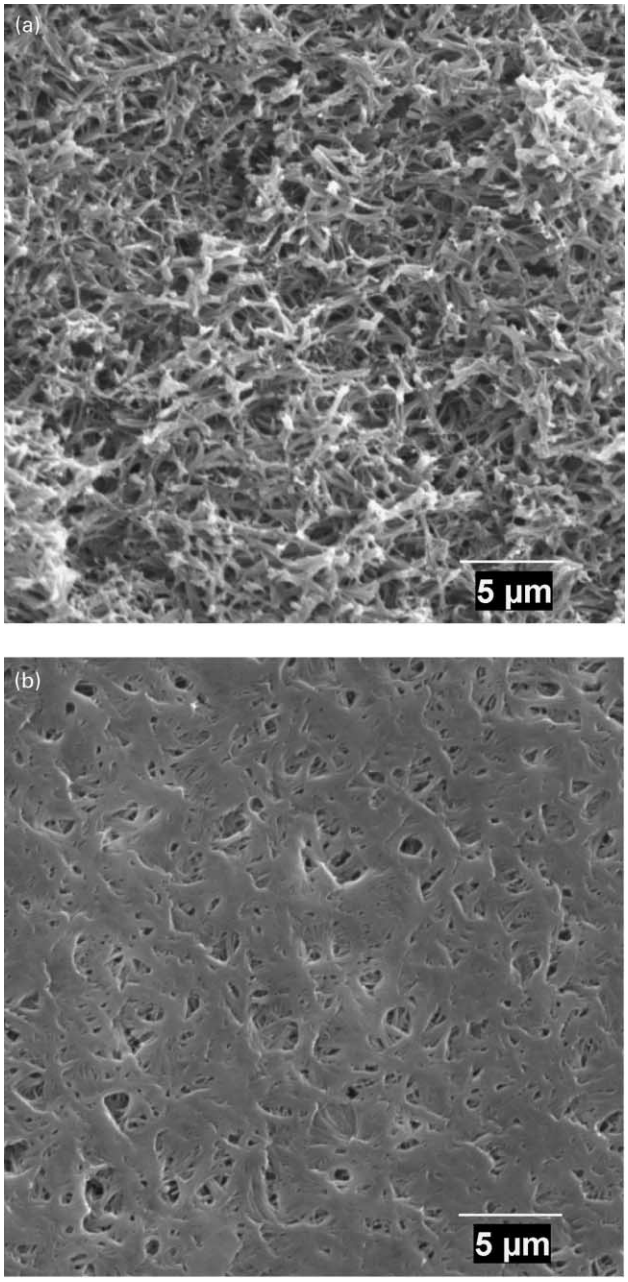

Fig. 5. SEM micrographs of Nylon 6 membrane formed with a CO_2 preconditioning pressure of 28.6 bar (30 min) and a final hold pressure of 104.4 bar. (a) cross section, 4000×. (b) top surface, 4000×.

pressure CO_2 (28.6 bar) is analogous to the phase inversion technique of creating an incipient dope, which is slightly supersaturated with respect to S–L demixing [19]. Such dope compositions contain an increased number of subcritical aggregates (nucleation sites with respect to crystallization). The phase inversion membranes resulting from these dopes often display an increased presence of crystallite structures surrounding the irregular cellular pores formed by the early stages of L–L phase separation [19]. At this preconditioning pressure, the decreased pore size suggests an increased amount of CO_2 present in the incipient

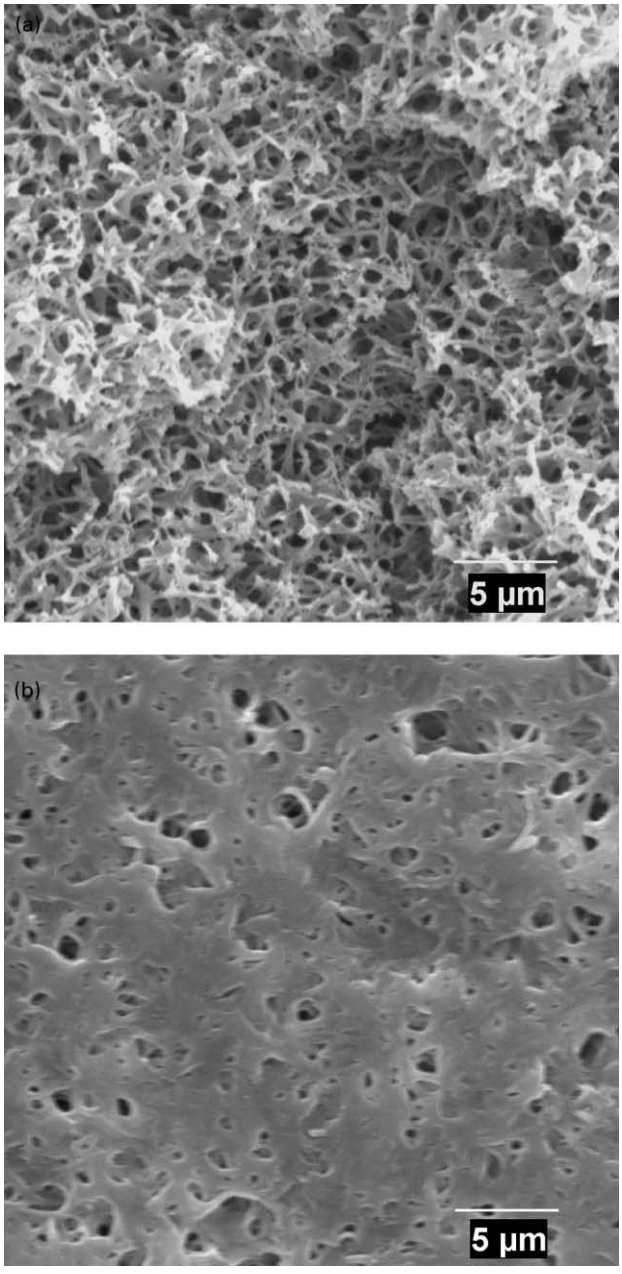

Fig. 6. SEM micrographs of Nylon 6 membrane formed with a CO_2 preconditioning pressure of 56.2 bar (30 min) and a final hold pressure of 104.4 bar. (a) cross section, 4000×. (b) top surface, 4000×.

dope, which is consistent with the phase behavior observed for CO_2-expanded organic solvents [29]. This higher concentration of CO_2 could result in a more rapid crystallization process, freezing the initial structures formed by L–L demixing at an earlier stage of phase separation.

The greater concentration of CO_2 dissolved in the cast film at a preconditioning pressure of 56.2 appears to have heightened the importance of L–L demixing leading to membranes with more pronounced cellular character and pore interconnectivity. Again, this is consistent with an effective increase in the antisolvent strength in the presence of greater amounts of dissolved CO_2. As discussed previously, the pressure changes were not instantaneous and pressure gradients may have contributed to the observed pore morphology. However, the effects of preconditioning and final pressure demonstrate the interplay between L–L and S–L demixing processes in membrane formation and how membrane morphology can be used to interpret subtle changes in the relative rates of these processes with varying processing conditions.

A more dramatic change in membrane morphology was observed by precipitation of the membrane in the presence of additional solvent (TFE) in the pressure vessel. This is analogous to the standard immersion precipitation technique of decreasing the strength of the nonsolvent coagulation bath by the introduction of solvent. The morphology of membranes cast in the presence of additional TFE (with a preconditioning step at 28.6 bar) indicated a drastically different phase separation mechanism (Fig. 7a), with large crystallite structures distributed uniformly over the cross section. No circular or cellular pores, indicative of L–L demixing, were observed. The top surface of the membrane revealed a relatively open structure, consisting of globular crystalline aggregates (Fig. 7b).

The concept of a soft coagulation bath, a bath which allows for the relatively slow exchange of solvent and nonsolvent [21], has been used to describe the observation of predominantly crystalline features in immersion precipitation membranes. The presence of excess TFE in the antisolvent phase is thought to have slowed the exchange between the solvent in the cast film and the surrounding CO_2 antisolvent. The reduced rate of exchange resulted in a slower initiation of the L–L demixing process. Thus, S–L demixing, which was thermodynamically favored, dominated the phase separation process. Excess TFE had a marked effect on the membrane preconditioned at lower pressure (28.6 bar), which was shown previously to enhance the relative rate of S–L demixing. However, excess TFE had virtually no effect on membranes formed by direct ramping, demonstrating the sensitivity of the demixing mechanism to pressurization conditions (SEM micrographs not shown).

The interpretations of morphology for the Nylon 6 membranes generated using compressed CO_2 are also applicable to similar membranes formed from another rapidly crystallizable polyamide, Nylon 4,6. Shown in Fig. 8 is a Nylon 4,6 membrane generated from a 9 wt% polymer solution in TFE using a direct pressurization cycle to 104.4 bar. The initial solution was very close to the solubility limit of the polymer and generated a tighter pore structure than was obtained with the Nylon 6 solutions. The pore structure appears to be initiated by L–L demixing followed by crystallization. It is interesting to note that similar morphological networks were observed by Luna-Bárcenas and coworkers upon spraying a dilute (0.5%) solution of PAN in DMF through a 50 μm nozzle into a CO_2 antisolvent continuum [5]. The kinetics of Nylon 4,6 crystallization are more rapid than most other crystallizable

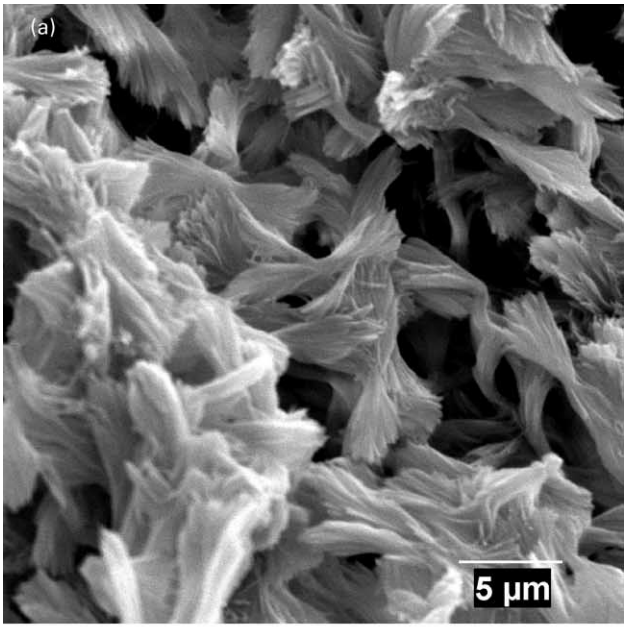

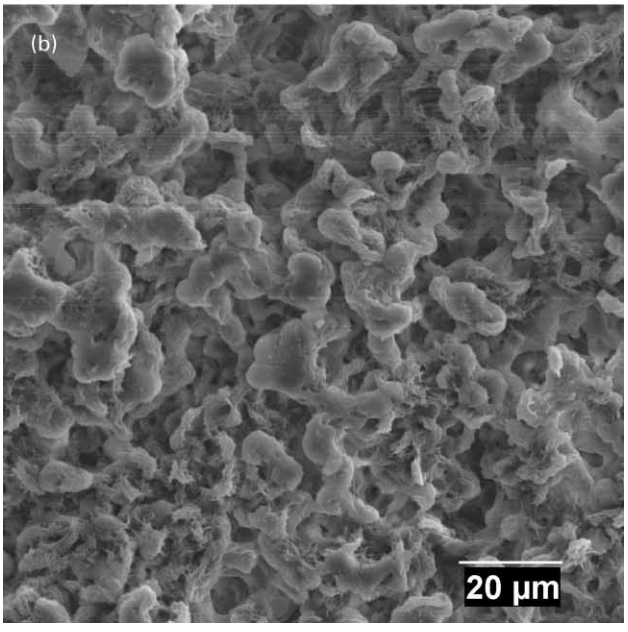

Fig. 7. SEM micrographs of Nylon 6 membrane formed with a CO_2 preconditioning pressure of 28.6 bar (30 min) and introduction of excess TFE in the pressure vessel. Final hold pressure of 104.4 bar CO_2. (a) cross section, 4000×. (b) top surface, 1000×.

nylons, suggesting the ability to lock in the nucleation and growth of the polymer poor phase earlier in the L–L demixing process.

4. Conclusions

The manipulation of the strengths of the solvent and nonsolvent is one of the primary means by which to control the properties of membranes formed by immersion precipitation. This work demonstrates the feasibility of using an additional variable, pressure, to tune the morphology of membranes formed by precipitation with a compressed antisolvent. The structural gradient and pore characteristics of Nylon 6 membranes precipitated from TFE using compressed CO_2 is well-described by a competition between L–L and S–L demixing, as in traditional immersion precipitation processes. Reducing the relative strengths of both the solvent and nonsolvent led to membrane pore structures dominated by crystallization (S–L demixing), the thermodynamically favored demixing process, rather than L–L demixing, which was kinetically favored.

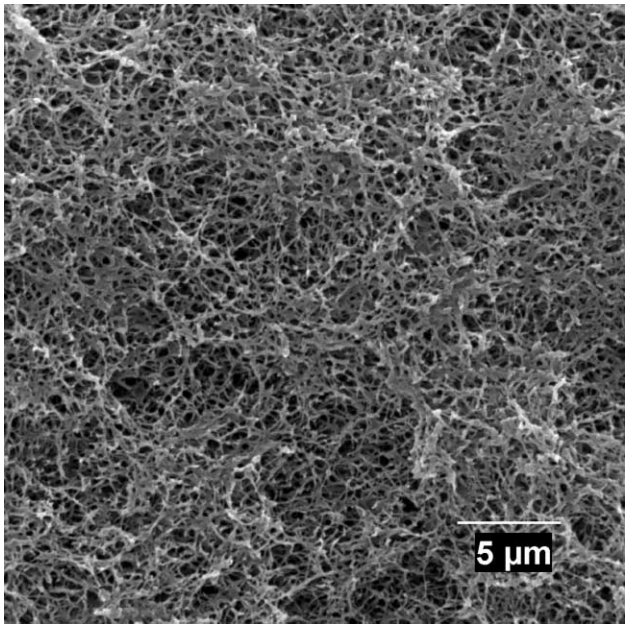

Fig. 8. SEM micrograph of a semicrystalline membrane formed from 9 wt% Nylon 4,6 solution in TFE; precipitated in an antisolvent environment of 104.4 bar CO_2 (cross section, 4000×).

Compressed antisolvent processes usually result in very rapid precipitation; therefore, the lack of structural gradients and asymmetric features in the membranes was surprising. However, this may largely be due to the method of introducing the compressed antisolvent, which was not instantaneous. In spite of the lack of gradient features, both L–L demixing-dominated structures and S–L demixing-dominated structures were achieved in a predictable manner using pressure as an additional membrane formation variable.

The success of this technique suggests an alternative CO_2-based method for the impregnation of solutes in polymers and the formation of polymer-based composites. Most current impregnation techniques rely on the ability of CO_2 to swell and plasticize the polymeric component. The CO_2 then acts as a carrier for a dissolved solute to impregnate the polymer. In contrast, this antisolvent method could be used to trap solutes and suspensions in a polymeric matrix based on the insolubility of these components in compressed CO_2. In both cases, decompression of the pressurized system is used to lock the solute into the polymer. Applications of this

technique for the production of solute-loaded polymers, polymer blends, and polymer-based composites for a variety of materials applications can be envisioned.

Acknowledgements

The authors would like to acknowledge the Petroleum Research Fund (PRF) for the funding of this research (32513-G9). A special note of thanks is extended to Larry Rice for his help and guidance in preparing the SEM micrographs. The assistance of Jeff Hoffman, Kevin McKinney and Timothy Chaffins in carrying out part of the experimental work, with funding from National Science Foundation REU program (DMR-9732302) is also duly noted.

References

[1] Falk R, Randolph T, Meyer JD, Kelly RM, Manning MC. J Controlled Release 1997;44:77–85.
[2] Reverchon E. J Supercrit Fluids 1999;15:1–21.
[3] Young TJ, Johnston KP, Mishima K, Tanaka H. J Pharm Sci 1999;88:640–50.
[4] Dixon DJ, Johnston KP, Bodmeir RA. AIChE J 1993;39:127–39.
[5] Luna-Bárcenas G, Kanakia SK, Sanchez IC, Johnston KP. Polymer 1995;36:3173–82.
[6] Yeo S, Debenedetti PG, Radosz M, Schmidt H. Macromolecules 1993;26:6207–10.
[7] Mawson S, Kanakia S, Johnston KP. Polymer 1997;38:2957–67.
[8] Aurora KA, Lesser AJ, McCarthy TJ. Macromolecules 1998;31:4614–20.
[9] Elkovitch MD, Tomasko DL, Lee LJ. Polym Engng Sci 1999; 39:2075–84.
[10] Berens AR, Huvard GS, Korsmeyer RW, Kunig FW. J Appl Polym Sci 1992;46:231–42.
[11] Kazarian SG, Vincent MF, Bright FV, Liotta CL, Eckert CA. J Am Chem Soc 1996;118:1729–36.
[12] Mulder M. Basic principles of membrane technology. Boston: Kluwer, 1996 (chapter 3).
[13] Bulte AMW, Naafs EM, Van Eeten F, Mulder MHV, Smolders CA, Strathmann H. Polymer 1996;37:1647–55.
[14] Smolders CA, Reuvers AJ, Boom RM, Wienk IM. J Membr Sci 1992;73:259–75.
[15] Suresh SJ, Enick RM, Beckman EJ. Macromolecules 1994;27:348–56.
[16] Cheng L, Dwan A, Gryte CC. J Polym Sci Phys Ed 1995;33:223–35.
[17] Van de Witte P, Dijkstra PJ, Van den Berg JWA, Feijen J. J Membr Sci 1996;117:1–31.
[18] Bulte AMW, Folkers B, Mulder MHV, Smolders CA. J Appl Polym Sci 1993;50:13–26.
[19] Cheng L, Dwan A, Gryte CC. J Polym Sci Polym Phys Ed 1995;33:211–22.
[20] Van de Witte P, Esselbrugge H, Dijkstra PJ, Van den Berg JWA, Feien J. J Membr Sci 1996;113:223–36.
[21] Young T, Lin D, Gau J, Chuang W, Cheng L. Polymer 1999;40:5011–21.
[22] Chiou JS, Barlow JW, Paul DR. J Appl Polym Sci 1985;30:3911–24.
[23] Handa YP, Roovers J, Wang F. Macromolecules 1994;27:5511–6.
[24] Lambert SM, Paulaitis ME. J Supercrit Fluids 1991;4:15–23.
[25] Zhang Z, Handa YP. Macromolecules 1997;30:8505–7.
[26] Van de Witte P, Van den Berg JWA, Feijen J, Reeve JL, McHugh AJ. J Appl Polym Sci 1996;61:685–95.
[27] Boom RM, Wienk IM, Van den Boomgaard Th, Smolders CA. J Membr Sci 1992;73:277–92.
[28] Kesting RE. J Appl Polym Sci 1990;41:2739–52.
[29] de la Fuente Badilla JC, Peters CJ, de Swaan Arons J. J Supercrit Fluids 2000;17:13–23.